Journal of Physiology (2002), **542.2**, *pp.* 383–393
DOI: 10.1113/jphysiol.2001.013382

www.jphysiol.org

Spatial characteristics of sarcoplasmic reticulum Ca^{2+} release events triggered by L-type Ca^{2+} current and Na^+ current in guinea-pig cardiac myocytes

Peter Lipp*†, Marcel Egger* and Ernst Niggli*

*Department of Physiology, University of Bern, Bühlplatz 5, 3012 Bern, Switzerland and †Institute for Molecular Cell Biology, University of the Saarland, Building 61, 66421 Homburg/Saar, Germany

Ca^{2+} signals in cardiac muscle cells are composed of spatially limited elementary events termed Ca^{2+} sparks. Several studies have also indicated that Ca^{2+} signals smaller than Ca^{2+} sparks can be elicited. These signals have been termed Ca^{2+} quarks and were proposed to result from the opening of a single Ca^{2+} release channel of the sarcoplasmic reticulum. We used laser-scanning confocal microscopy to examine the subcellular properties of Na^+ current (I_{Na})- and L-type Ca^{2+} current ($I_{Ca,L}$)-induced Ca^{2+} transients in voltage-clamped ventricular myocytes isolated from guinea-pigs. Both currents, I_{Na} and $I_{Ca,L}$, evoked substantial, global Ca^{2+} transients. To examine the spatiotemporal properties of such Ca^{2+} signals, we performed power spectral analysis of these Ca^{2+} transients and found that both lacked spatial frequency components characteristic for Ca^{2+} sparks. The application of 10 μM verapamil to partially block L-type Ca^{2+} current reduced the corresponding Ca^{2+} transients down to individual Ca^{2+} sparks. In contrast, I_{Na}-induced Ca^{2+} responses were still spatially homogeneous and lacked Ca^{2+} sparks even for small current amplitudes. By using high resistance patch pipettes (> 4 MΩ) to exaggerate the loss of voltage control during I_{Na}, Ca^{2+} sparks appeared superimposed on a homogeneous Ca^{2+} release component and were exclusively triggered during the flow of I_{Na}. In the presence of 10 μM ryanodine both $I_{Ca,L}$ and I_{Na} elicited small, residual Ca^{2+} transients that were spatially homogeneous but displayed distinctively different temporal profiles. We conclude that I_{Na} is indeed able to cause Ca^{2+} release in guinea-pig ventricular myocytes. In contrast to $I_{Ca,L}$-induced Ca^{2+} transients, which are built up from the recruitment of individual Ca^{2+} sparks, the I_{Na}-evoked cellular responses were always homogeneous, indicating that their underlying elementary Ca^{2+} release event is distinct from the Ca^{2+} spark. Thus, I_{Na}-induced Ca^{2+} transients are composed of smaller Ca^{2+} signals, most likely Ca^{2+} quarks.

(Received 9 October 2001; accepted after revision 30 April 2002)
Corresponding author P. Lipp: Institute for Molecular Cell Biology, University of the Saarland, Building 61, 66421 Homburg/Saar, Germany. Email: peter.lipp@uniklinik-saarland.de

Cardiac excitation–contraction coupling (E–C coupling) links the electrical excitation of the cell membrane, the action potential, to the mechanical activity of the contractile machinery (Callewaert, 1992; Bers, 2001). An important step during this signal transduction is a transient rise in the intracellular Ca^{2+} concentration ($[Ca^{2+}]_i$). This Ca^{2+} transient is composed of both, Ca^{2+} influx across the cell membrane and Ca^{2+} release from intracellular stores, the sarcoplasmic reticulum (SR). The precise contribution of each mechanism is dependent on the species (Bers, 2001) and on SR Ca^{2+} load (Han *et al.* 1994; Spencer & Berlin, 1995; Santana *et al.* 1997). Ca^{2+} entry through voltage-activated Ca^{2+} channels in the plasma membrane is believed to trigger the release of Ca^{2+} from the SR by a mechanism referred to as Ca^{2+}-induced Ca^{2+} release (CICR; for reviews see Callewaert, 1992; Niggli, 1999). The relaxation of cardiac myocytes is mediated by various Ca^{2+} transport processes. The two most important mechanisms responsible for the removal of Ca_i^{2+} are the SR Ca^{2+} pump and the Na^+–Ca^{2+} exchanger in the plasma membrane (for a recent review see Egger & Niggli, 1999; Lipp & Bootman, 1999). The plasma membrane Ca^{2+} pump removes a minor component, although the exact quantitative contributions again vary between different species (Bers, 2001).

The Na^+–Ca^{2+} exchange is a process controlled by the concentration gradients of both Na^+ and Ca^{2+} as well as the membrane voltage across the plasma membrane. This enables the exchanger to mediate Ca^{2+} extrusion in its 'forward mode' (i.e. Na^+ influx and Ca^{2+} efflux), but Ca^{2+} can also enter the cell during its 'reverse mode' of operation (Na^+ efflux and Ca^{2+} influx; e.g. Horackova & Vassort, 1979; Crespo *et al.* 1990). While it was known that slow and tonic Ca^{2+} entry can occur via Na^+–Ca^{2+} exchange, LeBlanc & Hume (1990) provided experimental evidence for the ability of the Na^+–Ca^{2+} exchange to trigger

fast SR Ca^{2+} release during E–C coupling. Their observation also implied the existence of a subsarcolemmal space with restricted diffusion, referred to as the 'fuzzy space', to which Ca^{2+} and Na^+ channels as well as the Na^+–Ca^{2+} exchanger have preferential access (Lederer *et al.* 1990*a*,*b*) and from which ions would only slowly diffuse into the cytoplasm. Activation of the fast I_{Na} is believed to lead to a short-lived accumulation of Na^+ in the 'fuzzy' space (model calculation revealed concentrations of up to 30 mM; Lederer *et al.* 1990*b*; see also Wendt-Gallitelli *et al.* 1993), which in turn would be sufficient to cause reverse-mode Na^+–Ca^{2+} exchange. It was postulated that this Ca^{2+} entry might be able to trigger SR Ca^{2+} release. Although evidence supporting such a sodium current (I_{Na})-induced Ca^{2+} release has subsequently been reported by others (e.g. Lipp & Niggli, 1994), this notion did not remain unquestioned. Instead, various experimental studies could not find I_{Na}-induced Ca^{2+} release under similar experimental conditions and proposed other mechanisms causing this phenomenon (see for example Sham *et al.* 1992; Bouchard *et al.* 1993; Sipido *et al.* 1995; Evans & Cannell, 1997).

One alternative explanation involved a loss of voltage control during the large cardiac I_{Na}, which can reach amplitudes of more than 10 nA (Makielski *et al.* 1987). The idea was that during I_{Na} voltage control is partly lost, which in turn accidentally activates $I_{Ca,L}$ (L-type Ca^{2+} current). Presumably, the resulting spurious Ca^{2+} entry could trigger SR Ca^{2+} release by CICR and I_{Na}-induced Ca^{2+} release could then be seen as an experimental artefact.

In the present paper, we examined the subcellular characteristics of SR Ca^{2+} release events induced by $I_{Ca,L}$ and I_{Na} with rapid line-scanning confocal microscopy of voltage-clamped guinea-pig ventricular myocytes. We show that both ionic currents recruit distinct and separate modes of SR Ca^{2+} release that can be distinguished based on their 'Ca^{2+} signalling fingerprint' and based on their pharmacological profile.

METHODS

Cell isolation and solutions

All experiments were carried out according to the Swiss Animal Protection Law and with the permission of The State Veterinary Office, Bern, Switzerland. Guinea-pig ventricular myocytes were isolated using a standard enzymatic procedure described previously (Lipp & Niggli, 1994). In brief, adult animals were killed by cervical dislocation, the heart rapidly removed and retrogradely perfused on a Langendorff perfusion system at 37 °C. The perfusion solution contained (mM): NaCl 135, KCl 5.4, $MgCl_2$ 1, NaH_2PO_4 0.33, Hepes 5, glucose 11, pH 7.3 adjusted with NaOH. After 5 min, collagenase B (Boehringer Mannheim, Rotkreuz, Switzerland) and protease type XIV (Sigma, Buchs, Switzerland) were added to a final concentration of 0.2 and 0.04 mg ml^{-1}, respectively, and the perfusion continued for another 4–6 min. Subsequently, the ventricles were minced and placed in perfusion solution containing 200 μM $CaCl_2$ on a rocking table to allow for dissociation of the tissue. Cells were taken from the supernatant, transferred into a recording chamber which was mounted on the stage of an inverted microscope (Diaphot TMD, Nikon, Küsnacht, Switzerland). Ca^{2+}-resistant cells readily adhered to the coverslip without coating and were constantly superfused (1–2 ml min^{-1}) with cellular solution containing (mM): NaCl, 135, KCl 5, $CaCl_2$ 2, glucose 10, $MgCl_2$ 2, Hepes 10 (pH 7.4 adjusted with NaOH). In order to inhibit L-type Ca^{2+} channels, verapamil was added (10 μM) from a stock solution. All experiments were performed at room temperature (20–22 °C). Extracellular solutions were exchanged by a custom-made solenoid-driven fast perfusion system (time for solution change < 500 ms).

Electrophysiological recordings

Single guinea-pig ventricular myocytes were voltage clamped in the whole-cell configuration of the patch-clamp technique. Patch pipettes were pulled from borosilicate glass on a horizontal puller (Zeitz, Augsburg, Germany). Filled with the intracellular solution, the pipettes had a final resistance of 1–2 MΩ. In some experiments we deliberately produced pipettes with a higher resistance of > 4 MΩ. The solutions used for filling the pipettes consisted of (mM): caesium aspartate 120, TEA-Cl 20, Hepes 10, MgATP 5, $MgCl_2$ 1, fluo-3 0.1, pH 7.2 adjusted with CsOH. Application of voltage pulses and recording of the membrane current was performed with an Axopatch 200 patch clamp amplifier (Axon Instruments, Foster City, CA, USA) controlled by custom-made software running under LabView (National Instruments, Ennetbaden, Switzerland). Residual 50 Hz noise was removed off-line by a custom-made routine based on IgorPro software (WaveMetrics, Lake Oswego, OR, USA).

Stimulation protocols

To ensure similar SR Ca^{2+} loading between cells, we employed a pre-pulse protocol. Ten voltage steps (250 ms in duration, at 0.5 Hz) from a holding potential of −50 to +10 mV were applied before stepping to the appropriate holding potential of −50 mV (for eliciting $I_{Ca,L}$) or −90 mV (for eliciting I_{Na}). For experiments in which $I_{Ca,L}$ was blocked by verapamil, the pre-pulse protocol comprised voltage steps (250 ms in duration, at 0.5 Hz) from −50 to +50 mV and thus used reverse-mode Na^+–Ca^{2+} exchange to load the SR.

Calcium measurements

The spatiotemporal properties of I_{Na}- and $I_{Ca,L}$-induced Ca^{2+} transients were examined using a laser-scanning confocal microscope (BioRad MRC 1000, Glattbrugg, Switzerland). Due to the limited temporal resolution of the confocal microscope in its image mode, we performed line-scanning at a rate of 500 lines s^{-1} as shown in Fig. 1. For this, a single line along the longitudinal cell axis was chosen and repetitively scanned. Data analysis was performed off-line on a Macintosh PowerPC 8100 computer (Apple, Walisellen, Switzerland) running a modified version of NIH-image (NIH, Bethesda, USA). Changes of Ca_i^{2+} were calculated using the self-ratio method as described earlier (Lipp & Niggli, 1994) assuming a K_d value for fluo-3 of 480 nM (Molecular Probes, Oregon, USA).

Digital image processing (see also Fig. 1)

For the power spectral analysis of the line-scan images, the IDL software package was used (Research Systems, Boulder, CO, USA). Initially, we calculated the Fourier transform (in space) of each individual line of the line-scan image as a two-dimensional array, whereby the order of the resulting line-data was preserved. Inhomogeneous distribution of fluo-3 fluorescence along the line

was compensated for by normalising each line in the power spectrum image by the zero-order component (P_0) (Cheng *et al.* 1993). We have shown recently that Ca^{2+} sparks can readily be identified in line-scan images by their characteristic spectral component in the lower spatial frequency range (Lipp & Niggli, 1996; for details see also Cannell *et al.* 1994). For the present paper, we averaged the low frequency components (between > 0 and < 0.13 lines μm^{-1}) and expressed them as normalised power ratio *vs.* time. In control line-scan images, we found that these low frequency components were a sufficiently sensitive indication for the presence of Ca^{2+} sparks in the raw data (not shown). The myocytes were scanned longitudinally; however, the sarcomeric periodicity was not apparent in the line-scan images and in the power spectral analysis. In this paper, we speak of homogeneous Ca^{2+} signals in the absence of any periodicity in the line-scan image. Nevertheless, noticeable non-periodic inhomogenieties were apparent in almost all line-scan recordings (e.g. Fig. 2*A*). The values were expressed as means ± S.E.M. Student's paired *t* tests were used to test for significance. Significance is given as $P < 0.05$ or < 0.1, as indicated in the figure legends.

RESULTS

Properties of $I_{Ca,L}$- but not I_{Na}-induced Ca^{2+} release were altered by verapamil

In voltage-clamped guinea-pig ventricular myocytes, stepping the membrane voltage from −50 to +5 mV or from −90 to −50 mV elicited $I_{Ca,L}$- or I_{Na}-induced Ca^{2+} release, respectively, that both caused a substantial increase in $[Ca^{2+}]_i$ (Fig. 2*A* and *C*). In Fig. 2 as well as the following figures, the $[Ca^{2+}]_i$ calculated from the line-scan images was coded in the height and the colour of 3D-surface representations in order to allow for a rapid assessment of the spatiotemporal properties of the sub-cellular Ca^{2+} transients. While the $I_{Ca,L}$-induced responses showed a rising phase lasting several milliseconds (Fig. 2*A*), the signals elicited by I_{Na} were characterised by a very brief upstroke (Fig. 2*C*). However, both transients appeared to be spatially uniform, i.e. Ca^{2+} release occurred evenly along

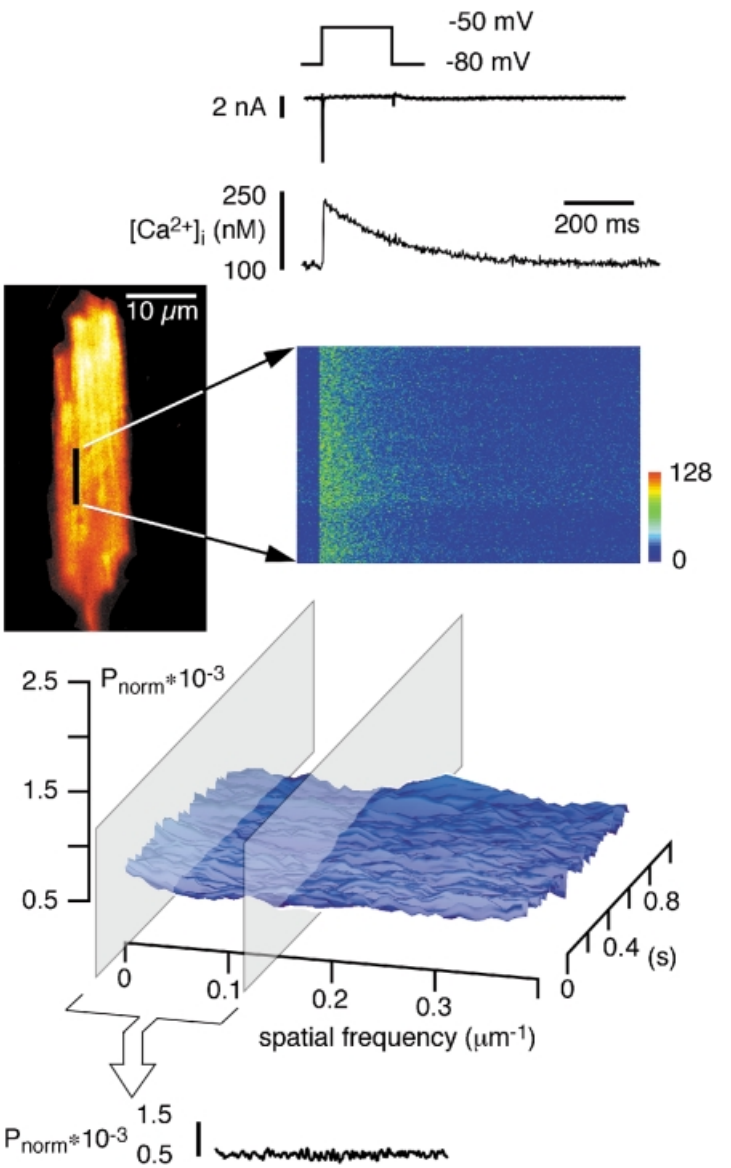

Figure 1. Power spectra of line-scan images (montage)

Traces show from top to bottom: voltage protocol, current recording, time course of average Ca^{2+} concentration, a confocal image of a fluo-3-loaded guinea-pig ventricular myocyte. The black line indicates the position of a single scanned line (longitudinal) to record fluorescence *vs.* time, shown in the right panel. A voltage-clamp depolarisation from −80 to −50 mV activated I_{Na} and a homogeneous Ca^{2+} influx signal. Power spectra in the spatial domain and the average power (average P_{norm}) over time (spatial low-frequency components averaged between > 0 and 0.13 lines μm^{-1}). Spatial uniformity of the Ca^{2+} release is confirmed in the power spectra. For this purpose, the raw line-scan images were Fourier transformed in the spatial domain (i.e. in the vertical direction) line by line and the calculated power spectra of all lines were arranged in an identical order to the original line-scan image. For normalisation the power of each frequency component (P_i) was divided by the zero-frequency component (P_0) to obtain P_{norm} (see Lipp & Niggli, 1996).

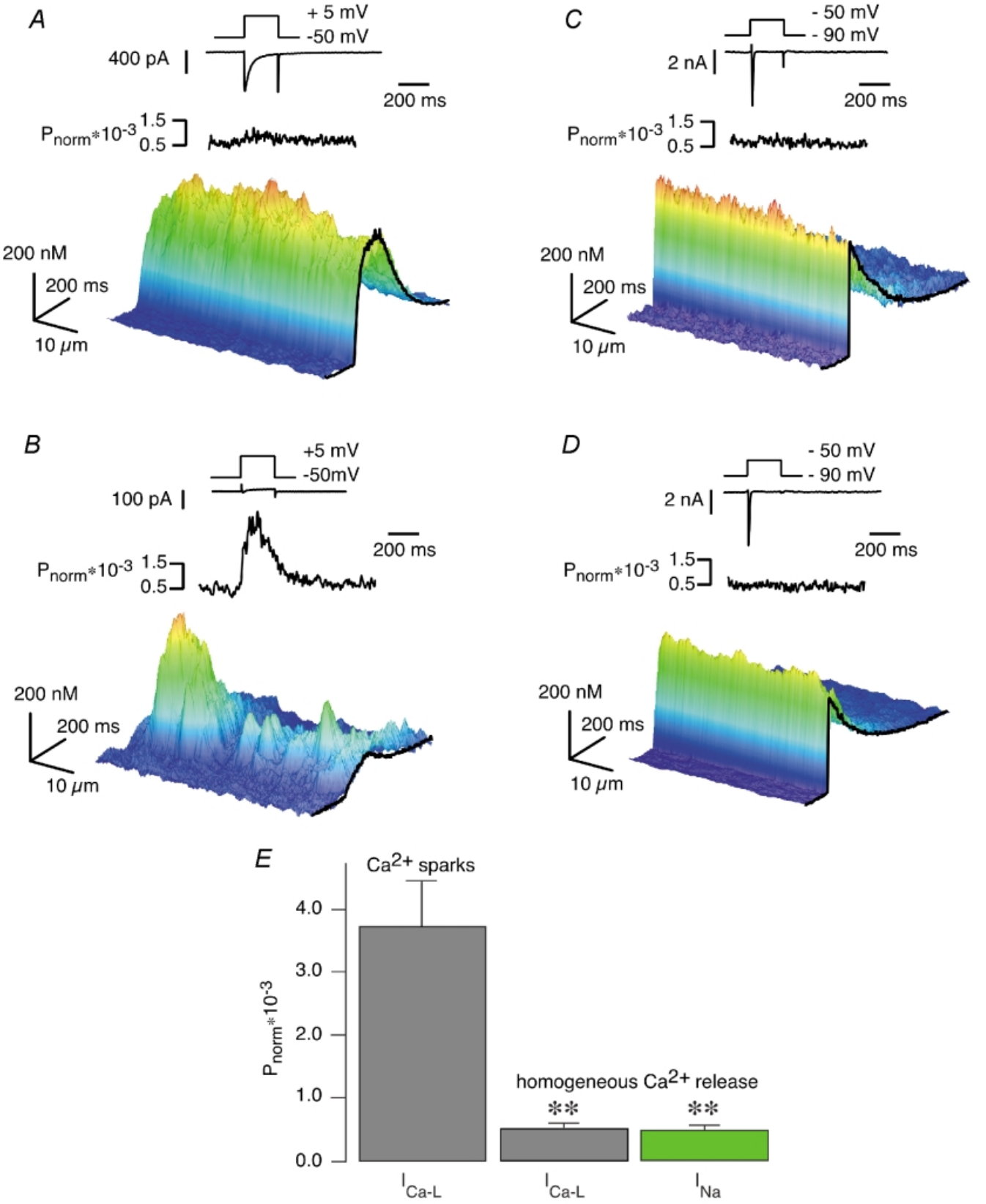

Figure 2. $I_{Ca,L}$- and I_{Na}-induced SR Ca^{2+} release

A–D, from top to bottom: voltage protocols for activating L-type Ca^{2+} currents (*A* and *B*) and sodium currents (*C* and *D*), the resulting $I_{Ca,L}$ and I_{Na}, the averaged power spectra in the spatial domain of the line-scan images and the Ca^{2+} signals as 3D-surface plots of the line-scan images. *B* and *D*, $I_{Ca,L}$ and I_{Na}, respectively, and the corresponding CICR signal observed in the same cardiac myocyte as in *A* and *C* after application of 10 μM verapamil for 2 min. *B*, although $I_{Ca,L}$ was reduced by approximately 95 %,

the recorded line. In order to substantiate this qualitative observation, we quantified the subcellular properties of the Ca^{2+} signals by calculating power spectra of the line scans, as described earlier (Lipp & Niggli, 1996). Particular attention was paid to the characteristic low spatial frequencies indicative of the appearance of detectable Ca^{2+} sparks (Cannell *et al.* 1994). For simplification, we averaged those spatial frequencies that were characteristic for the existence of Ca^{2+} sparks (between 0 and 0.13 lines μm^{-1}). The time course for the normalised power ratio present in this range of spatial frequencies is shown above the surface plot in this and all subsequent figures. The lack of abrupt time-dependent changes in this plot indicates the absence of identifiable Ca^{2+} sparks during both $I_{Ca,L}$- and I_{Na}-induced Ca^{2+} transients. Figure 2*B* and *D* shows current and Ca^{2+} recordings from the same cardiac myocyte after application of 10 μM verapamil for 2 min. Although the Ca^{2+} current was reduced by more than 95 % in *B*, SR Ca^{2+} release could still be elicited. In comparison to the control situation (Fig. 2*A*), the Ca^{2+} signal observed in the presence of verapamil was no longer homogeneous, instead it seemed to comprise a limited number of distinct Ca^{2+} sparks. This observation was substantiated by the power spectral analysis. During the voltage step a transient rise in the low-frequency components could be observed, suggesting the presence of Ca^{2+} sparks. In contrast to the recordings obtained during the activation of the $I_{Ca,L}$, the I_{Na}-induced Ca^{2+} signal was largely unaffected by verapamil (Fig. 2*D*). Despite a marginal decrease in the signal amplitude, the Ca^{2+} transient was still homogeneous, which was confirmed in the power spectral analysis by the absence of low frequency components. The results are summarised in Fig. 2*E*, where the power spectra of Ca^{2+} sparks (Fig. 2*B*) are compared with the power spectra of homogeneous SR Ca^{2+} signals induced by $I_{Ca,L}$ (Fig. 2*A*) and I_{Na} (Fig. 2*D*). There are several possible explanations for the slight decrease in the amplitude of the Ca^{2+} transient in the presence of verapamil. First, verapamil could have inhibited a contaminating $I_{Ca,L}$-induced Ca^{2+} signal present under control conditions. Second, Ca^{2+} loading of the SR might have been slightly lower than under control conditions, since Ca^{2+} entry through L-type Ca^{2+} channels was blocked during the pre-pulse protocol, although we largely relied on the loading of the SR by reverse-mode Na^+–Ca^{2+} exchange under those conditions (see Methods section). Third, verapamil has also been reported to slightly block I_{Na} (Bustamante, 1985) and the reverse mode of the Na^+–Ca^{2+} exchanger (Egger & Niggli, 1999).

From these experiments, we concluded that partial inhibition of $I_{Ca,L}$ could reduce the Ca^{2+} release signals from a homogeneous signal to a signal consisting of a few Ca^{2+} sparks, while the spatial properties of the I_{Na}-induced transients remained unaffected by verapamil. Since Ca^{2+} sparks cannot be resolved if their number is too large, the possibility exists that I_{Na} recruited too many Ca^{2+} sparks and thus prevented their identification as individual signalling events. Alternatively and more interestingly, I_{Na} could have triggered Ca^{2+} release from the SR with a different spatial signature (i.e. homogeneous SR Ca^{2+} release *vs.* Ca^{2+} sparks).

Na^+ current-induced SR Ca^{2+} release did not recruit Ca^{2+} sparks

To examine these possibilities, we used experimental conditions that were expected to facilitate the activation of a few L-type Ca^{2+} channels and the subsequent activation of Ca^{2+} sparks. In the first series of experiments, we elicited I_{Na} under conditions of deliberate loss of voltage control. For these experiments, we used patch-clamp electrodes with a slightly higher series resistance and we did not compensate for electrode resistance. Under such conditions, the membrane potential is known to escape towards the reversal potential for Na^+ during flow of I_{Na} (Hüser *et al.* 1996). Figure 3 depicts typical current and Ca^{2+} recordings from such an experiment and shows that the Ca^{2+} signals elicited under those conditions had lost their homogeneity. Similar transients were found in eight other cells studied under similar conditions. The spatial inhomogeneity can be read from the three-dimensional surface plot of the line-scan image and also from the transient surge of low frequencies in the power spectral analysis depicted in Fig. 3*A*. The Ca^{2+} transient seemed to consist of two superimposed components; the first one was an apparently homogeneous socket of Ca^{2+} and resembled the Na^+ current-induced Ca^{2+} signal seen in Fig. 2 while the second component resembled Ca^{2+} sparks. These two signal components are indeed compatible with the idea of a simultaneous activation of Na^+ and Ca^{2+} channels whereby the homogeneous signal is evoked by the Na^+ current-induced Ca^{2+} release while the Ca^{2+} sparks are triggered by the spurious activation of a few L-type Ca^{2+} channels during the brief loss of voltage control.

We verified this notion by applying verapamil that should, under these conditions, suppress only those Ca^{2+} signals originating from the activation of Ca^{2+} channels but not the homogeneous Ca^{2+} release signal triggered by I_{Na} and

inhomogeneous SR Ca^{2+} release was still present, characterised by low-frequency components of the power spectra. *D*, the I_{Na}-triggered SR Ca^{2+} release signal was largely homogeneous and verapamil insensitive. The power spectra exhibit no localised Ca^{2+} release events (Ca^{2+} sparks) in the low frequency range. *E*, comparison of the low-frequency components of the power spectra of $I_{Ca,L}$-induced SR Ca^{2+} signals in the presence of verapamil (*B*, Ca^{2+} sparks, $n = 21$) *vs.* the power spectra of homogeneous SR Ca^{2+} signals induced by $I_{Ca,L}$ (*A*, $n = 15$) and I_{Na}-induced Ca^{2+} transients (*D*, $n = 11$) (mean ± S.E.M., ** $P < 0.05$).

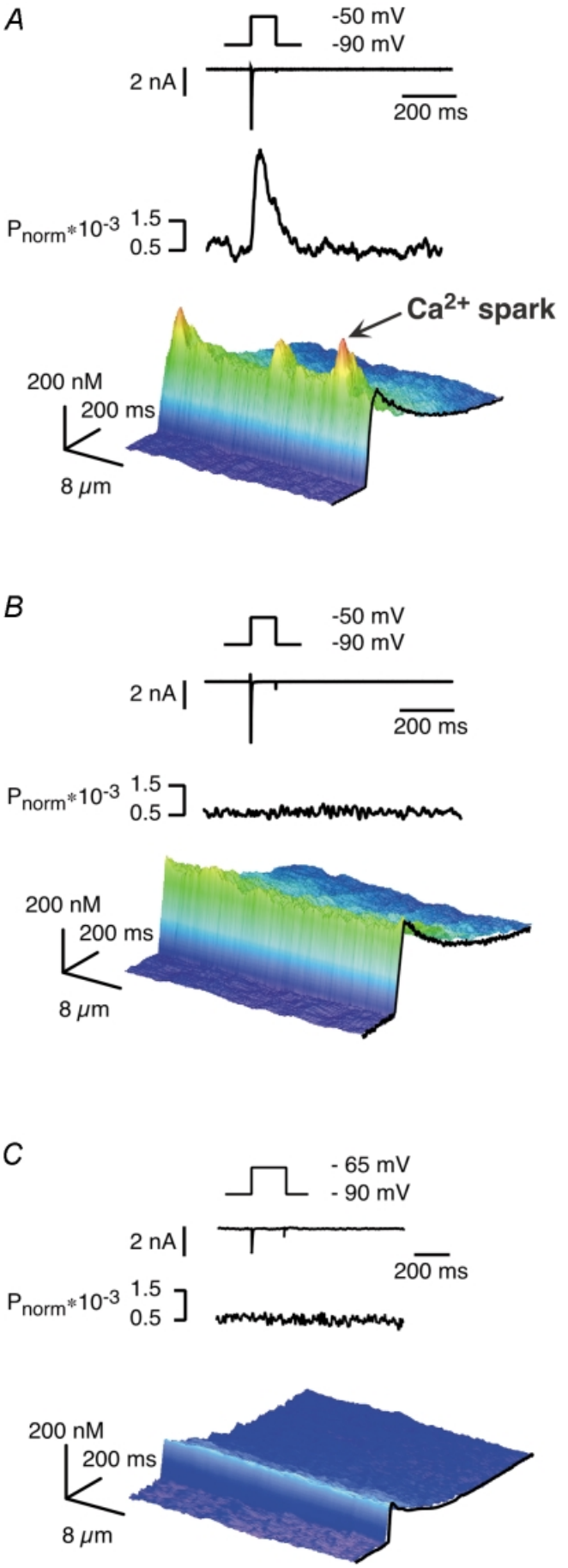

subsequent Na^+–Ca^{2+} exchange reverse mode. Figure 3*B* shows the result of a verapamil treatment of the same cell as in Fig. 3*A*. While the localised Ca^{2+} signals seen in the absence of the L-type Ca^{2+} channel blocker were suppressed, the homogeneous component of the Ca^{2+} signal was maintained. The suppression of inhomogeneities was again confirmed with the power spectral analysis. From these results we concluded that spurious activation of Ca^{2+} channels did not contribute to the homogeneous I_{Na}-induced SR Ca^{2+} release, but rather was responsible for the few clearly visible Ca^{2+} sparks positioned on top of the homogeneous Ca^{2+} signal.

The second question we addressed in this series of experiments was related to the nature of SR Ca^{2+} release induced by I_{Na}. We used an approach that was analogous to that applied for the identification of the elementary Ca^{2+} release events underlying $I_{Ca,L}$-induced Ca^{2+} release, a reduction of the number of activated channels. In the case of $I_{Ca,L}$ this can be achieved either by inhibiting Ca^{2+} channels or by depolarisations to the threshold of current activation (Cannell *et al.* 1994, 1995; Lopez-Lopez *et al.* 1995). For the I_{Na}-induced Ca^{2+} release we chose the second protocol by reducing the degree of depolarisation. A representative example of such a small voltage step (here to −65 mV) is shown in Fig. 3*C*. The traces were obtained from the same cell as in Fig. 3*A* and *B*. The resulting Ca^{2+} signal was reduced in amplitude by more than 70 %. Despite this change in the amplitude, the spatial properties of the release transient remained unaltered; it was still homogeneous. This important observation was confirmed

Figure 3. I_{Na}-induced SR Ca^{2+} release events (Ca^{2+} sparks)

A–C, from top to bottom: voltage protocols for activating sodium currents, the resulting I_{Na}, the averaged power spectra in the spatial domain and the corresponding Ca^{2+} signals as 3D-surface plots of the line-scan images. *A*, I_{Na} measured under conditions of loss of voltage control (patch electrodes with higher series resistance). The resulting inhomogeneous Ca^{2+} transient consisted of two superimposed components; a Ca^{2+} spark component and an apparently homogeneous I_{Na}-induced component. *B*, I_{Na} and the corresponding homogeneous SR Ca^{2+} release signal observed in the same cardiac myocyte after application of 10 μM verapamil for 2 min. In the presence of the L-type Ca^{2+} channel blocker only the Ca^{2+} spark components were suppressed, indicating that spurious activation of L-type Ca^{2+} channels did not contribute to the I_{Na}-induced SR Ca^{2+} release. *C*, I_{Na}-induced Ca^{2+} transients induced by decreasing the depolarisation (voltage step to −65 mV). The resulting Ca^{2+} signal was decreased compared to Fig. 2*B*. Nevertheless, the spatial properties of the homogeneous Ca^{2+} release transient remained unchanged. Similar results were found in all myocytes tested (n = 8).

for all voltages between −75 (the threshold potential for eliciting I_{Na} in our experiments) and −50 mV (data not shown). More positive depolarisations were not examined because of the risk of contaminating activation of $I_{Ca,L}$. From these findings we concluded that I_{Na}-induced Ca^{2+} release did not recruit Ca^{2+} sparks, instead Ca^{2+} release events were evoked that resulted in a homogeneous SR Ca^{2+} release signal over the entire voltage range.

Ca^{2+} release did not reflect the spatial properties of I_{Na} and $I_{Ca,L}$

We were left with the question of why I_{Na} and $I_{Ca,L}$ could recruit different elementary Ca^{2+} release events. Or in other words, does the I_{Na}- and $I_{Ca,L}$-induced Ca^{2+} release reflect the spatial properties of the Ca^{2+} influx signals or does the discrepancy arise from the recruitment of different populations of RyRs? In order to examine this, we analysed the subcellular characteristics of I_{Na}- and $I_{Ca,L}$-induced Ca^{2+} influx signals. Figure 4*A* and *B* depicts results from a guinea-pig ventricular myocyte in which SR Ca^{2+} release had been inhibited by preincubation of the cell in 10 μM ryanodine for 20 min, a procedure that completely eliminates Ca^{2+} release via RyRs (Bers, 2001). Depolarisations from holding potentials of −50 and −90 mV elicited $I_{Ca,L}$ and I_{Na}, respectively. The Ca^{2+} influx signal carried by $I_{Ca,L}$ had a slow rising and decay phase, as has been described earlier (Cannell *et al.* 1994). These Ca^{2+} influx signals were homogeneous over the entire voltage range tested (−30 to +30 mV, data not shown). We could not assess the subcellular properties of the Ca^{2+} signals for smaller or larger depolarisations since the resulting Ca^{2+} transients were too small to allow for a reliable power spectral

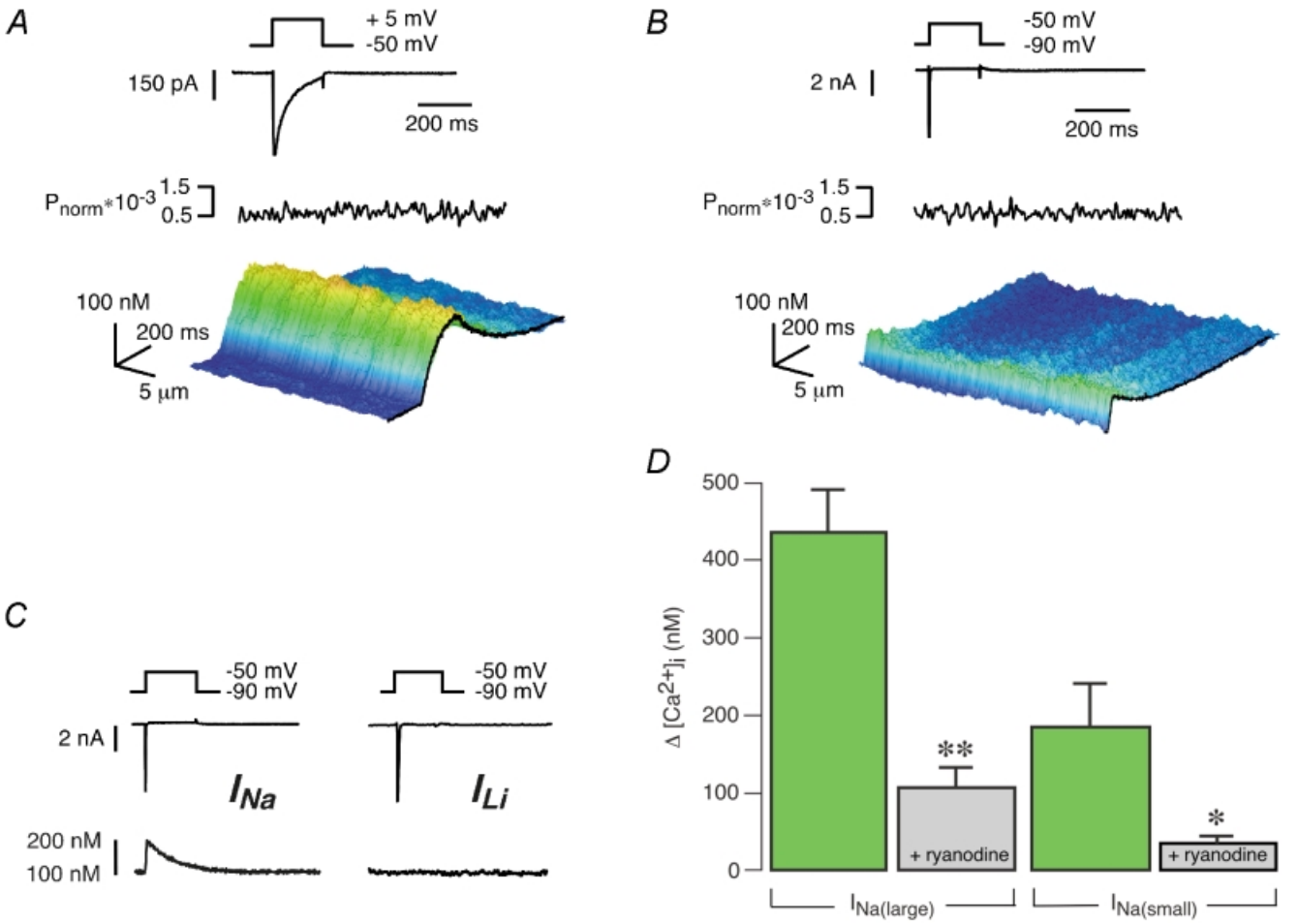

Figure 4. I_{Na}- and $I_{Ca,L}$-induced Ca^{2+} transients in the absence of SR Ca^{2+} release function

A and *B*, from topSR to bottom: voltage protocols for activating L-type Ca^{2+} currents and sodium currents, respectively, the resulting $I_{Ca,L}$ and I_{Na}, the averaged power spectra in the spatial domain and the resulting Ca^{2+} signals as 3D-surface plots of the line-scan images under conditions of blocked SR (myocytes were preincubated in 10 μM ryanodine for 20 min). *C*, I_{Na}-induced $[Ca^{2+}]_i$ transient most probably mediated by Ca^{2+} entry via Na^+–Ca^{2+} exchange; substitution of Li^+ for Na^+ resulted in a complete suppression of this Ca^{2+} influx signal during I_{Na}. *D*, I_{Na}-induced $[Ca^{2+}]_i$ transients: comparison of $[Ca^{2+}]_i$ changes induced by large I_{Na} (voltage steps from −90 to −50 mV) in control ($n = 25$) and ryanodine-treated myocytes ($n = 8$) and between $[Ca^{2+}]_i$ changes induced by small I_{Na} (voltage steps from −90 to −65 mV) in control ($n = 7$) and ryanodine-treated myocytes ($n = 5$; mean ± S.E.M., ** $P < 0.001$ *vs.* control large I_{Na}, * $P < 0.05$ *vs.* control small I_{Na}).

analysis. Membrane depolarisations from a holding potential of −90 to −50 mV elicited I_{Na} and an accompanying Ca^{2+} influx component (Fig. 4*B*). As shown previously, these I_{Na}-induced Ca^{2+} influx signals were insensitive to L-type Ca^{2+} channel inhibitors (Lipp & Niggli, 1994) and could therefore be attributed to the activation of I_{Na} and subsequent Ca^{2+} entry via Na^+–Ca^{2+} exchange. We verified this in experiments where we substituted Li^+ for Na^+, an intervention which resulted in a complete suppression of the Ca^{2+} influx transients during voltage protocols activating Na^+ channels (Fig. 4*C*). As for $I_{Ca,L}$, we could only test a narrow range of voltages eliciting I_{Na}, because of the limiting signal-to-noise ratio for the power spectral analysis (tested voltages: between −70 and −50 mV; data not shown). Figure 4*D* shows the statistical comparison of $[Ca^{2+}]_i$ transients induced by large (Fig. 4*B*) and small I_{Na} (Fig. 3*C*) in myocytes with intact and blocked SR Ca^{2+} release function (ryanodine-treated cells). In both cases, I_{Na} significantly triggered SR Ca^{2+} release. From these experimental results, we conclude that the spatial properties of the Ca^{2+} influx signals induced by the activation of I_{Na} and $I_{Ca,L}$ did not reflect the subcellular properties of the elementary Ca^{2+} release signals recruited by each particular current. Therefore, submicroscopic spatial features or the kinetics of the respective Ca^{2+} entry signals into the dyadic cleft may determine the type of subsequent SR Ca^{2+} release event that is activated (i.e. Ca^{2+} sparks or homogeneous release).

DISCUSSION

During the last few years, the established view of cardiac E–C coupling and Ca^{2+} signalling has been challenged by several unexpected experimental findings. Some of these observations appeared to suggest trigger pathways for CICR other than the well-known activation via L-type Ca^{2+} channels. This includes Ca^{2+} entry by reverse mode Na^+–Ca^{2+} exchange, particularly following activation of Na^+ influx via I_{Na} (LeBlanc & Hume, 1990; Lipp & Niggli, 1994). In some studies, depolarisation and the subsequent changes of the electrochemical gradients for Na^+ and Ca^{2+} appeared to be sufficient to elicit Na^+–Ca^{2+} exchange reverse mode (i.e. no Na^+ influx was required; Levi *et al.* 1994). A possible contribution of T-type Ca^{2+} current to triggering CICR has also been suggested in several reports (for example see Sipido *et al.* 1998). More recently, changes of Ca^{2+} signalling after β-adrenergic stimulation have been interpreted to arise from a reduced selectivity of the TTX-sensitive Na^+ channels with subsequent influx of Ca^{2+} ('slip-mode conductance'; Santana *et al.* 1998). Based on other experimental results, β-adrenergic stimulation was also proposed to unmask a direct allosteric coupling between L-type Ca^{2+} channels and RyRs, giving rise to voltage-induced Ca^{2+} release (Hobai *et al.* 1997; Ferrier *et al.* 1998; Howlett *et al.* 1998). None of these additional trigger pathways is fully understood and each has been disputed because of published negative results. A common conclusion of many papers reporting negative results was that the apparent additional trigger pathway might have resulted from an experimental artefact (Sham *et al.* 1992; Bouchard *et al.* 1993; Evans & Cannell, 1997; Sipido *et al.* 1997).

Homogeneous Ca^{2+} release is distinct from Ca^{2+} sparks

Similar to many other cell types, cardiac Ca^{2+} signalling and E–C coupling is notoriously complex. This partly results from the diversity of possible pathways for Ca^{2+} entry, including several types of voltage-dependent Ca^{2+} channels. In addition, Ca^{2+} transporters that usually remove cytosolic Ca^{2+}, such as the Na^+–Ca^{2+} exchanger, can run in a reverse or Ca^{2+} influx mode. Although some separation between these pathways can be achieved with specific voltage-clamp protocols, the voltage range over which activation or steady-state inactivation occurs shows considerable overlap between the different current components. Moreover, the available pharmacological tools are less than perfect, many show use- or voltage-dependent block or lack specificity. Therefore, experiments aimed at the identification of specific pathways need to be designed and analysed very carefully and the necessary control experiments need to be done.

However, some of the mentioned alternative pathways for Ca^{2+} entry can be ruled out for the present study. The pipette filling solution did not contain cAMP and the cells were not β-adrenergically stimulated. Thus, both voltage-activated Ca^{2+} release and slip-mode influx of Ca^{2+} would not be expected under the experimental conditions used. In addition, for the Ca^{2+} release signals observed here we can exclude T-type Ca^{2+} current as the underlying trigger, since the Ca^{2+} signals were selective for Na^+ over Li^+, which is more consistent with the Na^+–Ca^{2+} exchange as the underlying transporter. Taken together, the homogeneous Ca^{2+} release signals elicited by the activation of I_{Na} most probably resulted from activation of the Na^+–Ca^{2+} exchange in the Ca^{2+} influx mode, but, as discussed below, another possible complication had to be considered to further substantiate this conclusion.

The notion that reverse-mode Na^+–Ca^{2+} exchange is activated during I_{Na} and is subsequently able to trigger SR Ca^{2+} release, has been challenged in the past (Sham *et al.* 1992, Bouchard *et al.* 1993; Sipido *et al.* 1997). The issue is not yet resolved completely, but species differences in the expression of the Na^+–Ca^{2+} exchanger have been implied to be important (Sham *et al.* 1995). As another alternative, it was proposed that a pronounced loss of voltage control and the resulting voltage escape during the large I_{Na} may induce spurious activation of L-type Ca^{2+} channels, that in turn could have activated SR Ca^{2+} release (Evans & Cannell, 1997). By using a combination of whole-cell voltage-clamp and fluorescent potential-sensitive indicators, we

have previously been able to visualise the inevitable voltage escape during I_{Na} directly (Hüser *et al.* 1996). Furthermore, we found that in cells that had undergone β-adrenergic stimulation, spurious activation of L-type Ca^{2+} channels during voltage escape was indeed dramatically enhanced (DelPrincipe *et al.* 2000). We therefore had to account for such a possibility in the current study.

With the recent introduction of sophisticated fluorescence imaging techniques, in particular confocal microscopy, spatially restricted Ca^{2+} signals had been resolved, such as the Ca^{2+} sparks in muscle cells (for a review see Lipp & Niggli, 1996). These local Ca^{2+} signals exhibit well defined and easy to recognise spatial and temporal features (also referred to as 'Ca^{2+} signalling fingerprint'). In the present study, we took advantage of the confocal imaging technique to discriminate among different triggers and subsequent SR Ca^{2+} release signals.

The analysis of the 'Ca^{2+} signalling fingerprint' of Ca^{2+} sparks now allowed us to directly rule out such a possible artefact. Whenever the problem of voltage escape was present in our Ca^{2+} recordings, we could readily identify the evoked Ca^{2+} sparks, even if only a few L-type Ca^{2+} channels were activated. In experiments where we deliberately caused significant loss of voltage control (Fig. 3*A*), Ca^{2+} sparks appeared as superimposed Ca^{2+} signals on top of the homogeneous, I_{Na}-induced Ca^{2+} transient. Moreover, these additional local signals were only triggered during the short period of current flow via Na^+ channels and were sensitive to inhibition by verapamil, an inhibitor of L-type Ca^{2+} channels. Thus, these Ca^{2+} sparks were most likely triggered by spurious activation of L-type Ca^{2+} channels during voltage escape. Taken together, the 'Ca^{2+} signalling fingerprint' of the Ca^{2+} sparks allowed us to indirectly detect openings of a few L-type Ca^{2+} channels with a sensitivity far superior to the analysis of the voltage-clamp current traces. Therefore, we are left with the question: what is the nature of the homogeneous Ca^{2+} release signal following I_{Na}? It clearly arises from SR Ca^{2+} release since it was dramatically reduced after treatment with ryanodine (to eliminate CICR). Since it was spatially homogeneous irrespective of its amplitude, the elementary Ca^{2+} release events underlying this type of SR Ca^{2+} release were most likely smaller than a Ca^{2+} spark. In many respects, these signals resembled those observed following flash-photolytic activation of CICR in the same cell type (Lipp & Niggli, 1996). Based on those homogeneous Ca^{2+} release transients we had proposed the existence of a tiny Ca^{2+} release signal corresponding to the Ca^{2+} release flux via a single RyR, the Ca^{2+} quark. Using two-photon excitation photolysis of caged Ca^{2+}, we were later able to elicit Ca^{2+} signals arising from events exhibiting 20 to 40 times smaller release flux than a typical Ca^{2+} spark, possibly corresponding to such Ca^{2+} quarks (Lipp & Niggli, 1998; Niggli, 1999). Similar homogeneous Ca^{2+} release signals were also reported in skeletal muscle after suppression of Ca^{2+} sparks (Shirokova & Rios, 1997), where they were termed 'small event Ca^{2+} release'. Likewise, when the cardiac muscle isoform of the RyR (RyR2) was heterologously expressed in Chinese hamster ovary (CHO) cells, uniform Ca^{2+} release signals without noticeable Ca^{2+} sparks were recorded (Bhat *et al.* 1999). Taken together, the homogeneous Ca^{2+} release signals elicited by Na^+ current most likely arise from the initiation of a large number of unresolved Ca^{2+} quarks.

When comparing the amplification of the Ca^{2+} influx signals by CICR, I_{Na}-induced signals seem to be more efficient in triggering SR Ca^{2+} release. However, a direct comparison of the trigger efficiency of I_{Na} and $I_{Ca,L}$ is very difficult because of the vastly different durations of the two influx signals. While in the present experiments most of the Ca^{2+} influx resulting from I_{Na} served as a trigger for CICR, only the first few milliseconds of the $I_{Ca,L}$ are triggering release (Sham *et al.* 1998). The large remainder of the current only leads to refilling of the SR (Trafford *et al.* 2001). Thus, when only considering the Ca^{2+} influx during the first few milliseconds of $I_{Ca,L}$, the signal amplification and E–C coupling efficiency of this pathway is far superior.

The missing mechanism for RyR inactivation

Contemporary published computer models of Ca^{2+} signalling in the dyadic cleft do not seem to be able to account for the present findings. Generally, these models predict that opening of a single RyR channel results in a rapid spread of the Ca^{2+} signal within the dyadic cleft, reaching almost millimolar concentrations within less than a millisecond (Cannell & Soeller, 1997; Stern *et al.* 1999). Thus, all RyRs within a cluster of channels would rapidly become activated by CICR and the cluster would exhibit a high degree of positive feedback, essentially resulting in a stereotypical all-or-none response. This model prediction is, however, not only at odds with our observation of Ca^{2+} quarks, but also with more recent estimations of the number of channels participating in a Ca^{2+} spark. By recording single channel currents from L-type Ca^{2+} channels and the resulting Ca^{2+} signals simultaneously, the number of RyRs underlying a Ca^{2+} spark has been estimated to be in the range of four to six (Wang *et al.* 2001), which is surprising given the fact that freeze-fracture studies seemed to suggest a much larger number of feet per dyad (Franzini-Armstrong *et al.* 1999). Thus, it appears that the presently prevailing understanding of Ca^{2+} signalling in the dyadic cleft (and the computer models developed based on these ideas) are missing some important features. Most probably, we need to have a better conception for inhibitory mechanisms which may not only govern the degree of activation within a cluster of RyRs, but may also be in charge for the termination of Ca^{2+} release (Sham *et al.* 1998; DelPrincipe

et al. 1999). Unfortunately, the mechanisms linking the individual RyRs within a functional Ca^{2+} release unit are not at all clear. There is indirect evidence indicating that CICR may not be the only message these channels understand. For example, communication and synchronisation by allosteric interaction between the densely packed channel proteins has been proposed (Marx *et al.* 1998, 2001; Bers & Fill, 1998). In fact, such allosteric mechanisms could not only confer synchronised activation between adjacent channels, but could also communicate the inhibitory signals that seem to be required for both, partial activation of a cluster of RyRs (to account for Ca^{2+} quarks), as well as termination and stability of Ca^{2+} release (Stern *et al.* 1999).

REFERENCES

Bers, D. M. (2001). *Excitation–Contraction Coupling and Cardiac Contractile Force*. Kluwer Academic Publishers, Dordrecht, The Netherlands.

Bers, D. M. & Fill, M. (1998). Muscle contraction – Coordinated feet and the dance of ryanodine receptors. *Science* **281**, 790–791.

Bhat, M. B., Hayek, S. M., Zhao, J. Y., Zang, W. J., Takeshima, H., Wier, W. G. & Ma, J. J. (1999). Expression and functional characterization of the cardiac muscle ryanodine receptor Ca^{2+} release channel in Chinese hamster ovary cells. *Biophysical Journal* **77**, 808–816.

Bouchard, R. A., Clark, R. B. & Giles, W. R. (1993). Regulation of unloaded cell shortening by sarcolemmal sodium-calcium exchange in isolated rat ventricular myocytes. *Journal of Physiology* **469**, 583–599.

Bustamante, J. O. (1985). Block of sodium currents by the calcium antagonist D600 in human heart cell segments. *Pflügers Archiv* **403**, 225–227.

Callewaert, G. (1992). Excitation–contraction coupling in mammalian cardiac cells. *Cardiovascular Research* **26**, 923–932.

Cannell, M. B., Cheng, H. & Lederer, W. J. (1994). Spatial non-uniformities in $[Ca^{2+}]_i$ during excitation–contraction coupling in cardiac myocytes. *Biophysical Journal* **67**, 1942–1956.

Cannell, M. B., Cheng, H. & Lederer, W. J. (1995). The control of calcium release in heart muscle. *Science* **268**, 1045–1049.

Cannell, M. B. & Soeller, C. (1997). Numerical analysis of ryanodine receptor activation by L-type channel activity in the cardiac muscle diad. *Biophysical Journal* **73**, 112–122.

Cheng, H., Lederer, W. J. & Cannell, M. B. (1993). Calcium sparks: elementary events underlying excitation–contraction coupling in heart muscle. *Science* **262**, 740–744.

Crespo, L. M., Grantham, C. J. & Cannell M. B. (1990). Kinetics, stoichiometry and role of the Na–Ca exchange mechanism in isolated cardiac myocytes. *Nature* **345**, 618–621.

DelPrincipe, F., Egger, M. & Niggli, E. (1999). Calcium signalling in cardiac muscle: refractoriness revealed by coherent activation. *Nature Cell Biology* **1**, 323–329.

DelPrincipe, F., Egger, M. & Niggli, E. (2000). L-type Ca^{2+} current as the predominant pathway of Ca^{2+} entry during I_{Na} activation in β-stimulated cardiac myocytes. *Journal of Physiology* **527**, 455–466.

Egger, M. & Niggli, E. (1999). Regulatory function of Na–Ca exchange in the heart: Milestones and outlook. *Journal of Membrane Biology* **168**, 107–130.

Evans, A. M. & Cannell, M. B. (1997). The role of L-type Ca^{2+} current and Na^+ current-stimulated Na/Ca exchange in triggering SR release in guinea-pig cardiac ventricular myocytes. *Journal of Cardiovascular Research* **35**, 294–302.

Ferrier, G. R., Zhu, J., Redondo, I. M. & Howlett, S. E. (1998). Role of cAMP-dependent protein kinase A in activation of a voltage-sensitive release mechanism for cardiac contraction in guinea-pig myocytes. *Journal of Physiology* **513**, 185–201.

Franzini-Armstrong, C., Protasi, F. & Ramesh, V. (1999). Shape, size, and distribution of Ca^{2+} release units and couplons in skeletal and cardiac muscles. *Biophysical Journal* **77**, 1528–1539.

Han, S., Schiefer, A. & Isenberg, G. (1994). Ca^{2+} load of guinea-pig ventricular myocytes determines efficacy of brief Ca^{2+} currents as trigger for Ca^{2+} release. *Journal of Physiology* **480**, 411–421.

Hobai, I. A., Howarth, F. C., Pabbathi, V. K., Dalton, G. R., Hancox, J. C., Zhu, J. Q., Howlett, S. E., Ferrier, G. R. & Levi, A. J. (1997). 'Voltage-activated Ca release' in rabbit, rat and guinea-pig cardiac myocytes, and modulation by internal cAMP. *Pflügers Archiv* **435**, 164–173.

Horackova, M. & Vassort, G. (1979). Sodium–calcium exchange in regulation of cardiac contractility. Evidence for an electrogenic, voltage-dependent mechanism. *Journal of General Physiology* **73**, 403–424.

Howlett, S. E., Zhu, J. & Ferrier, G. R. (1998). Contribution of a voltage-sensitive calcium release mechanism to contraction in cardiac ventricular myocytes. *American Journal of Physiology* **274**, H155–170.

Hüser, J., Lipp, P. & Niggli, E. (1996). Confocal microscopic detection of potential-sensitive dyes used to reveal loss of voltage control during patch-clamp experiments. *Pflügers Archiv* **433**, 194–199.

LeBlanc, N. & Hume, J. R. (1990). Sodium current-induced release of calcium from cardiac sarcoplasmic reticulum . *Science* **248**, 372–376.

Lederer, W. J., Berlin, J. R., Cohen, N. M., Hadley, R. W., Bers, D. M. & Cannell, M. B. (1990*a*). Excitation–contraction coupling in heart cells. Roles of the sodium–calcium exchange, the calcium current, and the sarcoplasmic reticulum. *Annals of the New York Academy of Sciences* **588**, 190–206.

Lederer, W. J., Niggli, E. & Hadley, R. W. (1990*b*). Sodium–calcium exchange in excitable cells: fuzzy space. *Science* **248**, 283.

Levi, A. J., Spitzer, K. W., Kohmoto, O. & Bridge, J. H. B. (1994). Depolarization-induced Ca entry via Na–Ca exchange triggers SR release in guinea pig cardiac myocytes. *American Journal of Physiology* **266**, H1422–1433.

Lipp, P. & Bootman, M. D. (1999). The physiology and molecular biology of the Na/Ca exchange. In *Cardiac Electrophysiology,* ed. Zippe & Jalife, pp. 41–51. W. N. Saunders Company, Philadelphia, USA.

Lipp, P. & Niggli, E. (1994). Sodium current-induced calcium signals in isolated guinea-pig ventricular myocytes. *Journal of Physiology* **474**, 439–446.

Lipp, P. & Niggli, E. (1996). Submicroscopic calcium signals as fundamental events of excitation–contraction coupling in guinea-pig cardiac myocytes. *Journal of Physiology* **492**, 31–38.

Lipp, P. & Niggli, E. (1998). Fundamental calcium release events revealed by two-photon excitation photolysis of caged calcium in guinea-pig cardiac myocytes. *Journal of Physiology* **508**, 801–809.

Lopez-Lopez, J. R., Shacklock, P. S., Balke, C. W. & Wier, W. G. (1995). Local calcium transients triggered by single L-type calcium channel currents in cardiac cells. *Science* **268**, 1042–1045.

Makielski, J. C., Sheets, M. F., Hanck, D. A., January, C. T. & Fozzard, H. A. (1987). Sodium current in voltage clamped internally perfused canine cardiac Purkinje cells. *Biophysical Journal* **52**, 1–11.

Marx, S. O., Gaburjakova, J., Gaburjakova, M., Henrikson, C., Ondrias, K. & Marks, A. R. (2001). Coupled gating between cardiac calcium release channels (ryanodine receptors). *Circulation Research* **88**, 1151–1158.

Marx, S. O., Ondrias, K. & Marks, A. R. (1998). Coupled gating between individual skeletal muscle Ca^{2+} release channels (ryanodine receptors). *Science* **281**, 818–821.

Niggli, E. (1999). Localized intracellular calcium signaling in muscle: Calcium sparks and calcium quarks. *Annual Review of Physiology* **61**, 311–335.

Santana, L. F., Gomez, A. M. & Lederer, W. J. (1998). Ca^{2+} flux through promiscuous cardiac Na^+ channels: slip-mode conductance. *Science* **279**, 1027–1033.

Santana, L. F., Kranias, E. G. & Lederer, W. J. (1997). Calcium sparks and excitation–contraction coupling in phospholamban-deficient mouse ventricular myocytes. *Journal of Physiology* **480**, 411–421.

Sham, J. S. K., Cleemann, L. & Morad, M. (1992). Gating of the cardiac Ca^{2+} release channel: the role of Na^+ current and Na^+–Ca^{2+} exchange. *Science* **255**, 850–853.

Sham, J. S. K., Hatem, S. N. & Morad, M. (1995). Species differences in the activity of the Na^+–Ca^{2+} exchanger in mammalian cardiac myocytes. *Journal of Physiology* **488**, 623–631.

Sham, J. S. K., Song, L. S., Chen, Y., Deng, L. H., Stern, M. D., Lakatta, E. G. & Cheng, H. P. (1998). Termination of Ca^{2+} release by a local inactivation of ryanodine receptors in cardiac myocytes. *Proceedings of the National Academy of Sciences of the USA* **95**, 15096–15101.

Shirokova, N. & Rios, E. (1997). Small event Ca^{2+} release: a probable precursor of Ca^{2+} sparks in frog skeletal muscle. *Journal of Physiology* **502**, 3–11.

Sipido, K. R., Carmeliet, E. & Pappano, A. (1995). Na^+ current and Ca^{2+} release from the sarcoplasmic reticulum during action potentials in guinea-pig ventricular myocytes. *Journal of Physiology* **489**, 1–17.

Sipido, K. R., Carmeliet, E. & Van de Werf, F. (1998). T-type Ca^{2+} current as a trigger for Ca^{2+} release from the sarcoplasmic reticulum in guinea-pig ventricular myocytes. *Journal of Physiology* **508**, 439–451.

Sipido, K. R., Maes, M. & Van de Werf, F. (1997). Low efficiency of Ca^{2+} entry through the Na–Ca exchanger as trigger for Ca^{2+} release from the sarcoplasmic reticulum. A comparison between L-type Ca^{2+} current and reverse-mode Na–Ca exchange. *Circulation Research* **81**, 1034–1044.

Spencer, C. I. & Berlin, J. R. (1995). Control of sarcoplasmic reticulum calcium release during calcium loading in isolated rat ventricular myocytes. *Journal of Physiology* **488**, 267–279.

Stern, M. D., Song, L. S., Cheng, H. P., Sham, J. S. K., Yang, H. T., Boheler, K. R. & Rios, E. (1999). Local control models of cardiac excitation–contraction coupling – A possible role for allosteric interactions between ryanodine receptors. *Journal of General Physiology* **113**, 469–489.

Trafford, A. W., Diaz, M. E. & Eisner, D. A. (2001). Coordinated control of cell Ca^{2+} loading and triggered release from the sarcoplasmic reticulum underlies the rapid inotropic response to increased L-type Ca^{2+} current. *Circulation Research* **88**, 195–201.

Wang, S. Q., Song, L. S., Lakatta, E. G. & Cheng, H. P. (2001). Ca^{2+} signalling between single L-type Ca^{2+} channels and ryanodine receptors in heart cells. *Nature* **410**, 592–596.

Wendt-Gallitelli, M. F., Voigt, T. & Isenberg, G. (1993). Microheterogeneity of subsarcolemmal sodium gradients. Electron probe microanalysis in guinea-pig ventricular myocytes. *Journal of Physiology* **472**, 33–44.

Acknowledgements

This work was supported by the Swiss National Science Foundation for E.N. (3100-061442.00). We are grateful to D. Lüthi for technical assistance.